Inorganic Chemistry
Article
pubs.acs.org/IC

Comparisons of Plutonium, Thorium, and Cerium Tellurite Sulfates

Jian Lin,[‡] Justin N. Cross,[‡] Juan Diwu,[‡] Nathan A. Meredith,[‡] and Thomas E. Albrecht-Schmitt*[,†]

[†]Department of Chemistry and Biochemistry, Florida State University, 95 Chieftan Way, 310 DLC, Tallahassee, Florida 32306, United States

[‡]Department of Civil & Environmental Engineering & Earth Sciences and Department of Chemistry & Biochemistry, University of Notre Dame, 156 Fitzpatrick Hall, Notre Dame, Indiana 46556, United States

Supporting Information

ABSTRACT: The hydrothermal reaction of $PuCl_3$ or $CeCl_3$ with TeO_2 in the presence of sulfuric acid under the comparable conditions results in the crystallization of $Pu(TeO_3)(SO_4)$ or $Ce_2(Te_2O_5)(SO_4)_2$, respectively. $Pu(TeO_3)(SO_4)$ and its isotypic compound $Th(TeO_3)(SO_4)$ are characterized by a neutral layer structure with no interlamellar charge-balancing ions. However, $Ce_2(Te_2O_5)(SO_4)_2$ possesses a completely different dense three-dimensional framework. Bond valence calculation and UV−vis−NIR spectra indicate that the Ce compound is trivalent whereas the Pu and Th compounds are tetravalent leading to the formation of significantly different compounds. $Pu(TeO_3)(SO_4)$, $Th(TeO_3)(SO_4)$, and $Ce_2(Te_2O_5)(SO_4)_2$ represent the first plutonium/thorium/cerium tellurite sulfate compounds. Our study strongly suggests that the chemistries of Pu and Ce are not the same, and this is another example of the failure of Ce as a surrogate.

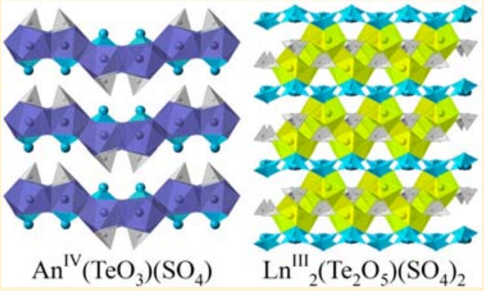

INTRODUCTION

The interest in comparing the chemistry of low oxidation state lanthanide and actinide stems from their similarities in ionic radii and coordination.[1] Lanthanide and actinide cations, such as cerium and plutonium, with same oxidation state and coordination number can possess nearly identical ionic radii.[1b] In oxo-anion compounds both lanthanide and actinide can be bonded to 7, 8, 9, or 10 oxygen atoms, yielding different coordination geometries based on square antiprism, pentagonal bipyramid, hexagonal bipyramid, tricapped trigonal prism, trigonal dodecahedra, distorted dodecahedra, capped triangular cupola, etc.[2] Lanthanides are used to simulate transuranium elements with low oxidation state to predict their behavior under long-term storage in repositories and transportation in the environment from contaminated sites.[3] For example, Ce^{IV} has long been used as a surrogate for Pu^{IV} owing to their nearly identical ionic radii.[4] In many cases, however, lanthanides are not proper mimics of transuranium elements both in solution and in the solid state.[5] Surprising coordination geometry differences were observed in Ce^{IV}- and Pu^{IV}-maltol complexes with respect to ligand orientation.[6] Studies about differences between lanthanide and actinides are still limited, and the rationale of using lanthanides as the surrogates of transuraniunm elements is still questionable.

Differentiating between low oxidation state lanthanides and actinides using geometrically versatile ligands as a structural probe provides a promising approach to study the differences between lanthanides and actinides. These ligands can bind metals in a variety of ways to form clusters, chains, sheets, or frameworks leading to a rich study of the coordination chemistry of lanthanide and actinides. Borate and phosphonate have been studied as the ligands to differentiate the differences between lanthanide and actinides.[2c,e,7] In the boric acid system, the reactions of lanthanide and actinide halides with boric acid under comparable synthetic parameters generate Ln^{III} and An^{III} borates with different coordination geometries and sheet topologies.[7,8] Electronic structure calculations with multi-reference, CASSCF, and density functional theory (DFT) methods suggest that the observed differences in the compositions and structures are attributed to real differences in bonding and not simply a function of changes in ionic radii.[7a] In the phosphonate system, the Ce^{IV} compound has lower solubility than the Np^{IV} and Pu^{IV}.[8] In this study, tellurite was chosen because it has stereochemically active lone pair electrons on the Te^{IV} center, which results in a large variability of coordination environments and properties.[9] Tellurite anions can be further interconnected to form dimers, trimers, and polymeric structures, which enable a variety of unusual structures.[10] For example, novel infinite tellurite tubes with lone-pair self-containment have been hydrothermally synthesized.[11] Unusual uranyl tellurites containing $[Te_2O_6]^{4-}$ ions and 3D networks have been observed in uranyl tellurites.[12] Our research efforts have successfully given rise to two families of Pu, Ce, or Zr tellurite halides, which are cationic extended materials with unusual coordination environments of the metal centers.[13]

Herein, we report the preparation, structure elucidation, and absorption spectra of plutonium, thorium, and cerium tellurite sulfate $Pu(TeO_3)(SO_4)$, $Th(TeO_3)(SO_4)$, and $Ce_2(Te_2O_5)(SO_4)_2$ which were prepared hydrothermally. The reaction of $CeCl_3$ with TeO_2 under comparable conditions as $PuCl_3$

Received: October 11, 2012
Published: March 25, 2013

dx.doi.org/10.1021/ic302216y | *Inorg. Chem.* 2013, 52, 4277−4281

produces completely different crystal structures with the Pu^{IV} in $Pu(TeO_3)(SO_4)$ and Ce^{III} in $Ce_2(Te_2O_5)(SO_4)_2$. More significantly, the reaction chemistry of Ce and Pu is shown to be different as Pu^{III} oxidizes to Pu^{IV} even under inert conditions whereas Ce^{III} remains Ce^{III} in air and Ce^{IV} reduces to Ce^{III} in air.

■ EXPERIMENTAL SECTION

Synthesis. $Th(NO_3)_4{\cdot}5H_2O$ (98%, International Bio-Analytical Industries), $CeCl_3$ (99.5%, Alfa-Aesar), CeO_2 (99.99%, Alfa-Aesar), TeO_2 (99.99%, Alfa-Aesar), and NH_4OH (28.0−30.0%, Alfa-Aesar) were all used as received. Weapons-grade plutonium (94% ^{239}Pu, 6% ^{240}Pu) in the form of $PuCl_3$ was used as received from LANL. Reactions were run in PTFE-lined Parr 4749 autoclaves with a 23 mL internal volume for the thorium/cerium and 10 mL internal volume autoclaves for plutonium. Distilled water with was used in all reactions. ***Caution!*** *^{239}Pu ($t_{1/2}$ = 24 065 years), and ^{240}Pu ($t_{1/2}$ = 6 537 years) represent serious health risks owing to their α and γ emission. All studies with plutonium were conducted in a laboratory dedicated to studies on transuranium elements. This laboratory is located in a nuclear science facility and is equipped with HEPA filtered hoods and negative pressure gloveboxes that are ported directly into the hoods. A series of counters continually monitor radiation levels in the laboratory. The laboratory is licensed by the Nuclear Regulatory Commission. All experiments were carried out with approved safety operating procedures. All free-flowing solids are worked with in gloveboxes, and products are only examined when coated with either water or Krytox oil and water. There are significant limitations in accurately determining yield with plutonium compounds because this requires drying, isolating, and weighing a solid, which poses certain risks, as well as manipulation difficulties given the small quantities employed in the reactions.*

$Pu(TeO_3)(SO_4)$. $PuCl_3$ (0.0295 mmol, 0.0100 g), TeO_2 (0.0589 mmol, 0.0094 g), argon-sparged 1 M H_2SO_4 solution (0.0589 mmol, 59 μL), and argon-sparged water (241 μL) were loaded into a 10 mL autoclave. The autoclave was sealed and heated to 230 °C in a box furnace in an argon-filled glovebox for 3 days. The autoclave was then cooled to room temperature at a rate of 5 °C/h. The products were rinsed with DI water, and pale red tablets were isolated.

$Th(TeO_3)(SO_4)$. Amorphous $Th(OH)_4$ was precipitated with NH_4OH from a 1.25 mL solution of $Th(NO_3)_4{\cdot}5H_2O$ (0.25 mmol, 0.1425 g) in water.[14] The precipitate was washed several times with DI water and dried at 90 °C in a 23 mL autoclave. TeO_2 (0.5 mmol, 0.0798 g), 1 M H_2SO_4 solution (500 μL), and argon-sparged water (2042 μL) were loaded into the autoclave. The autoclave was sealed and heated to 230 °C for 3 days followed by slow cooling to room temperature at a rate of 5 °C/h. The products were washed with DI water to remove soluble solids, followed by rinsing with methanol. The products consist of colorless block crystals of $Th(TeO_3)(SO_4)$.

$Ce_2(Te_2O_5)(SO_4)_2$. $Ce_2(Te_2O_5)(SO_4)_2$ can be synthesized using $Ce^{III}Cl_3$ or $Ce^{IV}O_2$ as the starting material. $CeCl_3$ (0.25 mmol, 0.0616 g), TeO_2 (2 mmol, 0.3192 g), 1 M H_2SO_4 (500 μL), and argon-sparged water (2042 μL) were loaded into a 23 mL PTFE-lined autoclave linear. $Ce_2(Te_2O_5)(SO_4)_2$ can also be synthesized using CeO_2 (1 mmol, 0.1682 g), TeO_2 (2 mmol, 0.3192 g), and 1 M H_2SO_4 (2 mL). The autoclave was sealed and heated to 230 °C for 3 days followed by slow cooling to room temperature at a rate of 5 °C/h. The products were washed with DI water to remove soluble solids, followed by rinsing with methanol. $Ce_2(Te_2O_5)(SO_4)_2$ crystallize into colorless tablet crystals. Photographs of all three sets of crystals can be found in Supporting Information.

Crystallographic Studies. Single crystals of all compounds were mounted on CryoLoops with Krytox oil and optically aligned on a Bruker APEXII Quazar X-ray diffractometer using a digital camera. Initial intensity measurements were performed using an IμSX-ray source, a 30 W microfocused sealed tube (Mo Kα, λ = 0.710 73 Å) with high-brilliance and high-performance focusing Quazar multilayer optics. Standard APEXII software was used for determination of the unit cells and data collection control. The intensities of reflections of a sphere were collected by a combination of four sets of exposures (frames). Each set had a different φ angle for the crystal, and each exposure covered a range of 0.5° in ω. A total of 1464 frames were collected with an exposure time per frame of 20−60 s, depending on the crystal. The SAINT software was used for data integration including Lorentz and polarization corrections. Semiempirical absorption corrections were applied using the program SADABS or TWINABS. Selected crystallographic information is listed in Table 1. Atomic coordinates and additional structural information are provided in the Supporting Information (CIFs).

Table 1. Crystallographic Data for $Pu(TeO_3)(SO_4)$, $Th(TeO_3)(SO_4)$, and $Ce_2(Te_2O_5)(SO_4)_2$

	$Pu(TeO_3)(SO_4)$	$Th(TeO_3)(SO_4)$	$Ce_2(Te_2O_5)(SO_4)_2$
formula mass	513.66	503.70	403.78
color	red	colorless	colorless
habit	block	prism	tablet
space group	$P2_1/c$	$P2_1/c$	$P2_1/c$
a (Å)	7.4789(5)	7.5329(8)	9.597(3)
b (Å)	13.5521(10)	13.8290(15)	6.9391(18)
c (Å)	5.4927(4)	5.6448(6)	8.248(2)
α (deg)	90.000	90.000	90.00
β (deg)	109.097(1)	109.587(1)	106.452(3)
γ (deg)	90.000	90.000	90.00
V (Å^3)	526.07(6)	554.01(10)	526.8(2)
Z	4	4	4
T (K)	100(2)	100(2)	100(2)
λ (Å)	0.710 73	0.710 73	0.710 73
max 2θ (deg)	27.440	27.470	27.690
ρ_{calcd} (g cm^{-3})	6.485	6.039	5.091
μ (cm^{-1})	18.339	32.432	14.429
$R(F)^a$	0.0207	0.0187	0.0405
$R_w(F_o{}^2)^b$	0.0468	0.0475	0.1138

[a] $R(F) = \Sigma||F_o| - |F_o||/\Sigma|F_o|$. [b] $R_w(F_o^2)=[\Sigma[w(F_o^2 - F_c^2)^2]/\Sigma wF_o^4]^{1/2}$.

UV−Vis−NIR Spectroscopy. UV−vis−NIR data were acquired from single crystals using a Craic Technologies microspectrophotometer. Crystals were placed on quartz slides under Krytox oil, and the data was collected from 200 to 1400 nm.

■ RESULTS AND DISCUSSION

Synthesis. The reaction of $PuCl_3$ or $CeCl_3$ with TeO_2 under comparable conditions generates two compounds with distinct structures and different oxidation state of the metal centers. Both plutonium and cerium metals can be trivalent and tetravalent.[15] In $Pu(TeO_3)(SO_4)$ and $Th(TeO_3)(SO_4)$, Pu and Th are tetravalent even though $Pu(TeO_3)(SO_4)$ was synthesized using $Pu^{III}Cl_3$ as the starting material. The redox potential for Pu^{IV}/Pu^{III} is 0.76 V/NHE in 1 M H_2SO_4.[16] Pu^{IV} is the favored valence under ambient conditions, and oxygen from air can easily oxidize Pu^{III} to Pu^{IV}.[1a] To avoid oxygen, the Pu reaction was performed in an argon-filled glovebox and all solutions used were sparged with argon, which suggests the valence transition could be attributed to the pH conditions and possibly a solubility driven mechanism.[2a,b,8] The presence of $Th(TeO_3)(SO_4)$, which is isotypic to $Pu(TeO_3)(SO_4)$, further confirms the valence of Pu because Th occurs exclusively in the tetravalent state in nature.[1a] The redox potential for Ce^{IV}/Ce^{III} is 1.44 V/NHE in 1 M H_2SO_4, and Ce^{III} is the preferred valence state in an acidic environment.[17] The reactions of both trivalent cerium chloride and tetravalent cerium oxide with TeO_2 in sulfuric acid yield the same product, $Ce_2(Te_2O_5)(SO_4)_2$ with trivalent metal centers.

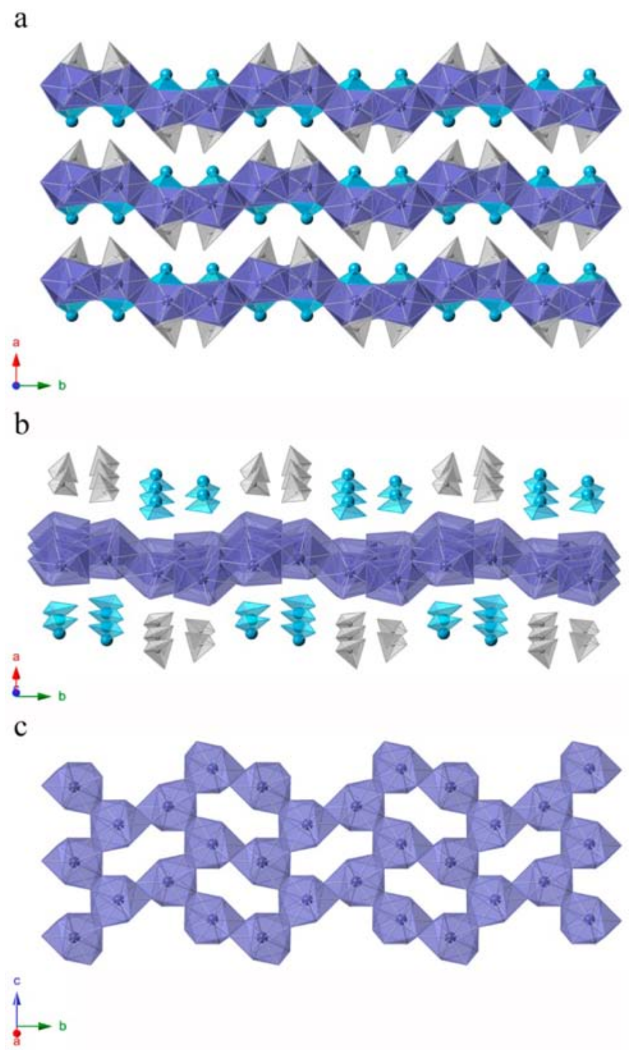

Figure 1. (a) View of $AnTeO_3SO_4$ showing the neutral charged layers extending down the *c* axis. (b) Depiction of one $AnTeO_3SO_4$ layer which is composed An-oxo sheet, TO_3^{2-}, and SO_4^{2-} polyhedra. (c) An-oxo sheet. An polyhedra are shown in blue-violet, TO_3^{2-} polyhedra in light-blue, SO_4^{2-} polyhedra in gray.

Table 2. Selected Bond Distances for $Pu(TeO_3)(SO_4)$, $Th(TeO_3)(SO_4)$, and $Ce_2(Te_2O_5)(SO_4)_2$

	$Pu(TeO_3)(SO_4)$	$Th(TeO_3)(SO_4)$		$Ce_2(Te_2O_5)(SO_4)_2$
An(1)–O(1)	2.113(4)	2.216(3)	Ce(1)–O(2)	2.442(13)
An(1)–O(2)	2.321(4)	2.416(3)	Ce(1)–O(3)	2.466(8)
An(1)–O(2)	2.379(4)	2.436(3)	Ce(1)–O(3)	2.506(8)
An(1)–O(3)	2.408(4)	2.481(3)	Ce(1)–O(4)	2.467(8)
An(1)–O(3)	2.480(4)	2.521(3)	Ce(1)–O(5)	2.511(7)
An(1)–O(4)	2.452(4)	2.520(3)	Ce(1)–O(6)	2.559(7)
An(1)–O(6)	2.524(4)	2.587(3)	Ce(1)–O(6)	2.593(7)
An(1)–O(7)	2.578(4)	2.662(3)	Ce(1)–O(7)	2.700(8)
An(1)–O(7)	2.443(4)	2.489(3)	Ce(1)–O(7)	2.539(7)
S(1)–O(4)	1.463(4)	1.463(3)	S(1)–O(4)	1.455(8)
S(1)–O(5)	1.443(4)	1.437(4)	S(1)–O(5)	1.458(8)
S(1)–O(6)	1.493(4)	1.488(3)	S(1)–O(6)	1.488(8)
S(1)–O(7)	1.504(4)	1.515(3)	S(1)–O(7)	1.494(7)
Te(1)–O(1)	1.852(4)	1.833(3)	Te(1A)–O(1)	2.02(2)
Te(1)–O(2)	1.890(4)	1.885(3)	Te(1A)–O(2)	1.93(2)
Te(1)–O(3)	1.900(4)	1.900(3)	Te(1A)–O(3)	1.850(11)
			Te(1B)–O(1)	2.18(2)
			Te(1B)–O(2)	2.005(18)
			Te(1B)–O(3)	1.867(12)
			Te(1C)–O(1)	1.88(2)
			Te(1C)–O(2)	2.17(3)
			Te(1C)–O(3)	1.804(14)

Structures and Topological Descriptions. Materials with layered structures are typically anionic/cationic in nature with cations/anions as the interlamellar charge-balancing ions.[18] In this study, however, isotypic compounds $Pu(TeO_3)(SO_4)$ and $Th(TeO_3)(SO_4)$ possess neutral layers with no charge-balancing ions between the layers. Figure 1a shows the depiction of the layers that extend along the *c* axis. Within each layer, paired TeO_3^{2-} and SO_4^{2-} polyhedra either corner-share or edge-share with metal centers alternatively, forming zigzagging layered structures (cf. Figure1b). The metal center is a nine-coordinate tricapped trigonal prism where four O atoms are donated from sulfate and five O atoms are donated from tellurite moieties (cf. Figure 3). The average An–O bond lengths in $Pu(TeO_3)(SO_4)$ and $Th(TeO_3)(SO_4)$ are 2.411 and 2.481 Å, respectively. Selected bond distances are given in Table 2. Bond valence calculations resulted in values of 3.929 for Pu and 4.069 for Th, which suggest the tetravalent nature of the metal centers.[19] Three O atoms (O4, O6, O7) from SO_4^{2-} anions coordinate with the metal ions, and the remaining O5 atom points into interlamellar space. Contrasting sulfate, all the O atoms (O1, O2, O3) from the TeO_3^{2-} anions participate in the coordination with the metal centers. The AnO_9 polyhedra edge-share with three other AnO_9 polyhedra, forming the An-oxo sheets (cf. Figure 1c).

The reaction of $CeCl_3$ with TeO_2 under comparable conditions as $PuCl_3$ yields a completely different structure with a dense three-dimensional framework (cf. Figure 2a). This 3D framework is broken down into $Ce^{III}–SO_4^{2-}$ layers and tellurite layers (cf. Figure 2b). Within the $Ce^{III}–SO_4^{2-}$ layer, SO_4^{2-} polyhedra share one edge and two corners with the Ce center. All O atoms (O4, O5, O6, and O7) of SO_4^{2-} participate in the coordination. The Ce center is a nine-coordinate tricapped trigonal prism where six O atoms are donated from SO_4^{2-} anions and three O atoms from tellurite anions (cf. Figure 3). The average metal–oxygen bond length is 2.531 Å, and selected bond distances are given in Table 2. Bond valence calculations resulted in value 2.813 for Ce which confirm the trivalent state of Ce in this compound.[19] The CeO_9 polyhedra also share three edges with three other Ce centers, but form a remarkably different zigzagging skeleton from that of $AnTeO_3SO_4$ (cf. Figure 2c). The Ce-SO_4^{2-} layers are connected together by tellurite layers. Within the tellurite layer, Te atoms

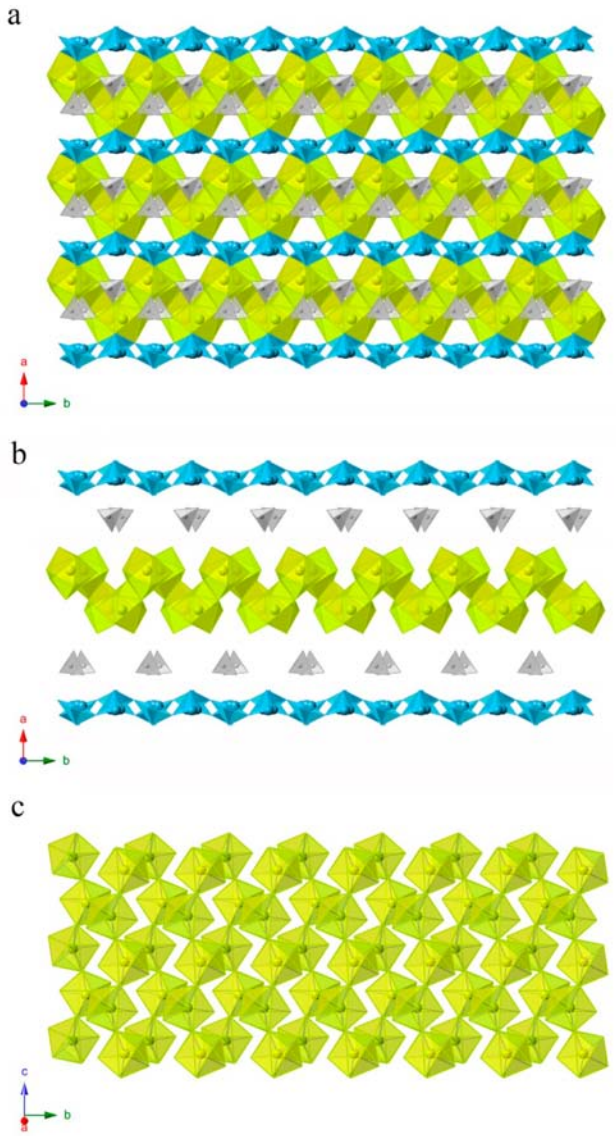

Figure 2. (a) View of $Ce_2(Te_2O_5)(SO_4)_2$ showing the dense 3D frameworks. (b) Depiction of one $Ce_2(Te_2O_5)(SO_4)_2$ 3D framework which is composed cerium sheet, tellurite layer, and SO_4^{2-} polyhedra. (c) Cerium-oxo sheet. Ce polyhedra are shown in yellow, TO_3^{2-} polyhedra in light-blue, SO_4^{2-} polyhedra in gray.

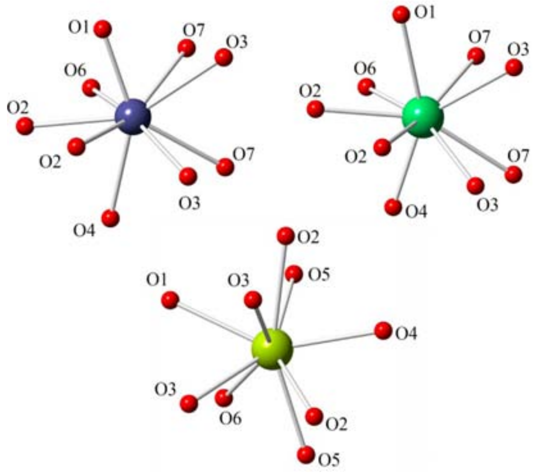

Figure 3. Tricapped trigonal prism coordination geometries of the Pu^{IV}, Th^{IV}, and Ce^{III} centers. The Pu^{IV} center is blue-violet sphere, the Th^{IV} center is green sphere, the Ce^{III} center is yellow sphere, and the O atoms are in red spheres.

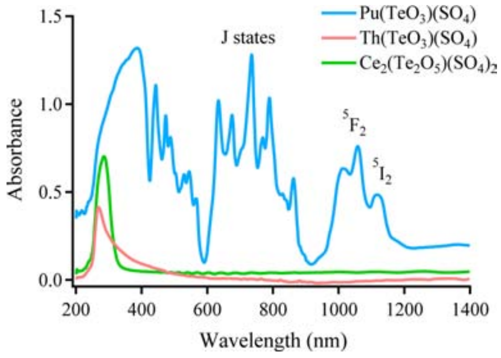

Figure 4. (a) UV−vis−NIR spectra of $Pu(TeO_3)(SO_4)$, $Th(TeO_3)(SO_4)$, and $Ce_2(Te_2O_5)(SO_4)_2$. The spectrum of $Pu(TeO_3)(SO_4)$ showing the assigned peaks for different f−f transitions (the $^5F_2$ + $^5I_6$ peaks centered at 1100 nm are signature peaks of the Pu^{IV}; at wavelengths <909 nm, multiple *J* values contribute).

are highly disordered which are delocalized into three independent Te atoms with a total occupancy of 1. Three of the O atoms (O1, O2, and O3) bonded to tellurium are also disordered and with one of them being half occupied.

UV−Vis−NIR Absorption Spectroscopy. The absorption spectra for $Pu(TeO_3)(SO_4)$, $Th(TeO_3)(SO_4)$, and $Ce_2(Te_2O_5)(SO_4)_2$ were obtained from single crystals of each compound and are shown in Figure 4. The existence of Pu^{IV} in $Pu(TeO_3)(SO_4)$ can be confirmed by the UV−vis−NIR spectrum. The $^5F_2$ + $^5I_6$ peaks centered near 1100 nm are signature peaks of Pu^{IV}. At wavelengths less than 900 nm, the transitions are due to multiple J states and have not been deconvoluted, but the transitions match well with the spectra reported by Carnall.[20] Th^{IV} has empty 5f orbital and does not exhibit any f−f transitions in the absorption spectra. The peaks ranging from 200 to 400 nm are ascribed to the Te−O charge transfer based on the measurement of TeO_2 crystal. Ce^{III} has one 4f electron, and the absorption near 300 nm in the spectra of $Ce_2(Te_2O_5)(SO_4)_2$ likely corresponds to delocalization of the $4f^1$ electrons.[2g] Te−O charge transfer could also contribute to the absorption.

■ CONCLUSIONS

In this study, the tellurite-sulfate system was selected to differentiate between low oxidation state lanthanides and actinides. The hydrothermal reaction of $PuCl_3$ with TeO_2 in sulfuric acid forms $Pu^{IV}(TeO_3)(SO_4)$, characterizing a neutral layer structure with no charge-balancing ions between the layers. The reaction of $CeCl_3$ with TeO_2 in sulfuric acid under comparable conditions yields $Ce^{III}_2(Te_2O_5)(SO_4)_2$. This compound possesses a completely different dense three-dimensional framework from $Pu(TeO_3)(SO_4)$. Bond valence calculation and UV−vis−NIR spectrum suggest the tetravalent oxidation state of Pu in $Pu(TeO_3)(SO_4)$. The presence of $Th(TeO_3)(SO_4)$, which is isotypic to $Pu(TeO_3)(SO_4)$, further confirms Pu^{IV} in $Pu(TeO_3)(SO_4)$. Cerium in $Ce_2(Te_2O_5)(SO_4)_2$, however, is trivalent based on the bond valence calculation, and if Ce^{IV} is used as a starting material it will reduce to Ce^{III} to form $Ce_2(Te_2O_5)(SO_4)_2$, which stands as a marked contrast from the Pu reaction. $Pu(TeO_3)(SO_4)$, $Th(TeO_3)(SO_4)$, and $Ce_2(Te_2O_5)(SO_4)_2$ represent the first plutonium/thorium/cerium tellurite sulfate compounds. This study is part of the growing evidence that Pu is not always identical with Ce and is another example of the failure of Ce as a surrogate.[21] Investigations are underway to prepare americium, curium, and other lanthanide compounds. The hope would be that future theory will be able to account for the differences in structure and valence.

■ ASSOCIATED CONTENT

Ⓢ Supporting Information

X-ray crystallographic files in CIF format and photographs of the crystals. This material is available free of charge via the Internet at http://pubs.acs.org.

■ AUTHOR INFORMATION

Corresponding Author

*E-mail: talbrechtschmitt@gmail.com.

Notes

The authors declare no competing financial interest.

■ ACKNOWLEDGMENTS

This material is based upon work supported as part of the Materials Science of Actinides, an Energy Frontier Research Center funded by the U.S. Department of Energy, Office of Science, Office of Basic Energy Sciences under Award Number DE-SC0001089. This work was supported by a Chinese Scholarship Council Graduate Fellowship to J.L.

■ REFERENCES

(1) (a) Edelstein, N. M.; Fuger, J.; Morss, L. R. *The Chemistry of the Actinide and Transactinide Elements*; Springer: New York, 2010. (b) Shannon, R. *Acta Crystallogr., Sect. A* **1976**, *32*, 751−767.

(2) (a) Diwu, J.; Wang, S.; Liao, Z.; Burns, P. C.; Albrecht-Schmitt, T. E. *Inorg. Chem.* **2010**, *49*, 10074−10080. (b) Diwu, J.; Nelson, A.-G. D.; Wang, S.; Campana, C. F.; Albrecht-Schmitt, T. E. *Inorg. Chem.* **2010**, *49*, 3337−3342. (c) Cross, J. N.; Villa, E. M.; Wang, S.; Diwu, J.; Polinski, M. J.; Albrecht-Schmitt, T. E. *Inorg. Chem.* **2012**, *51*, 8419−8424. (d) Diwu, J.; Good, J. J.; Di, S. V. H.; Albrecht-Schmitt, T. E. *Eur. J. Inorg. Chem.* **2011**, 1374−1377. (e) Diwu, J.; Nelson, A.-G. D.; Albrecht-Schmitt, T. E. *Comments Inorg. Chem.* **2010**, *31*, 46−62. (f) Wang, S.; Villa, E. M.; Diwu, J.; Alekseev, E. V.; Depmeier, W.; Albrecht-Schmitt, T. E. *Inorg. Chem.* **2011**, *50*, 2527−2533. (g) Sykora, R. E.; Deakin, L.; Mar, A.; Skanthakumar, S.; Soderholm, L.; Albrecht-Schmitt, T. E. *Chem. Mater.* **2004**, *16*, 1343−1349. (h) Salvadó, M. A.; Pertierra, P.; Trobajo, C.; García, J. R. *J. Am. Chem. Soc.* **2007**, *129*, 10970−10971. (i) Mihalcea, I.; Henry, N.; Clavier, N.; Dacheux, N.; Loiseau, T. *Inorg. Chem.* **2011**, *50*, 6243−6249. (j) Henry, N.; Lagrenée, M.; Loiseau, T.; Clavier, N.; Dacheux, N.; Abraham, F. *Inorg. Chem. Commun.* **2011**, *14*, 429−432.

(3) (a) Wang, X.; Zhou, X.; Du, J.; Hu, W.; Chen, C.; Chen, Y. *Surf. Sci.* **2006**, *600*, 478−483. (b) Skanthakumar, S.; Antonio, M. R.; Wilson, R. E.; Soderholm, L. *Inorg. Chem.* **2007**, *46*, 3485−3491. (c) De Almeida, L.; Grandjean, S.; Vigier, N.; Patisson, F. *Eur. J. Inorg. Chem.* **2012**, *2012*, 4986−4999.

(4) (a) Kim, H. S.; Joung, C. Y.; Lee, B. H.; Oh, J. Y.; Koo, Y. H.; Heimgartner, P. *J. Nucl. Mater.* **2008**, *378*, 98−104. (b) Suzuki, Y.; Nankawa, T.; Francis, A. J.; Ohnuki, T. *Radiochim. Acta* **2010**, *98*, 397−402.

(5) (a) Gaunt, A. J.; Reilly, S. D.; Enriquez, A. E.; Scott, B. L.; Ibers, J. A.; Sekar, P.; Ingram, K. I. M.; Kaltsoyannis, N.; Neu, M. P. *Inorg. Chem.* **2007**, *47*, 29−41. (b) Tan, X. L.; Fang, M.; Wang, X. K. *Molecules* **2010**, *15*, 8431−8468.

(6) Szigethy, G.; Xu, J.; Gorden, A. E. V.; Teat, S. J.; Shuh, D. K.; Raymond, K. N. *Eur. J. Inorg. Chem.* **2008**, *2008*, 2143−2147.

(7) (a) Polinski, M. J.; Grant, D. J.; Wang, S.; Alekseev, E. V.; Cross, J. N.; Villa, E. M.; Depmeier, W.; Gagliardi, L.; Albrecht-Schmitt, T. E. *J. Am. Chem. Soc.* **2012**, *134*, 10682−10692. (b) Polinski, M. J.; Wang, S.; Cross, J. N.; Alekseev, E. V.; Depmeier, W.; Albrecht-Schmitt, T. E. *Inorg. Chem.* **2012**, *51*, 7859−7866.

(8) Diwu, J.; Wang, S.; Good, J. J.; DiStefano, V. H.; Albrecht-Schmitt, T. E. *Inorg. Chem.* **2011**, *50*, 4842−4850.

(9) Devillanova, F. A. *Handbook of Chalcogen Chemistry New Perspectives in Sulfur, Selenium and Tellurium*; RSC Publishing: Cambridge, U.K., 2007.

(10) Mao, J.-G.; Jiang, H.-L.; Kong, F. *Inorg. Chem.* **2008**, *47*, 8498−8510.

(11) Johnston, M. G.; Harrison, W. T. A. *J. Am. Chem. Soc.* **2002**, *124*, 4576−4577.

(12) Almond, P. M.; McKee, M. L.; Albrecht-Schmitt, T. E. *Angew. Chem., Int. Ed.* **2002**, *41*, 3426−3429.

(13) (a) Lin, J.; Diwu, J.; Cross, J. N.; Villa, E. M.; Albrecht-Schmitt, T. E. *Inorg. Chem.* **2012**, *51*, 10083−10085. (b) Lin, J.; Cross, J. N.; Diwu, J.; Polinski, M. J.; Villa, E. M.; Albrecht-Schmitt, T. E. *Inorg. Chem.* **2012**, *51*, 11949−11954.

(14) Wilson, R. E.; Skanthakumar, S.; Knope, K. E.; Cahill, C. L.; Soderholm, L. *Inorg. Chem.* **2008**, *47*, 9321−9326.

(15) Cotton, S. *Lanthanide and Actinide Chemistry*; Wiley: NewYork, 2006.

(16) Gupta, R.; Guin, S. K.; Aggarwal, S. K. *RSC Adv.* **2012**, *2*, 1810−1819.

(17) Wadsworth, E.; Duke, F. R.; Goetz, C. A. *Anal. Chem.* **1957**, *29*, 1824−1825.

(18) (a) Fei, H.; Pham, C. H.; Oliver, S. R. J. *J. Am. Chem. Soc.* **2012**, *134*, 10729−10732. (b) Geng, F.; Ma, R.; Sasaki, T. *Acc. Chem. Res.* **2010**, *43*, 1177−1185. (c) Fei, H.; Oliver, S. R. J. *Angew. Chem., Int. Ed.* **2011**, *50*, 9066−9070. (d) Geng, F.; Matsushita, Y.; Ma, R.; Xin, H.; Tanaka, M.; Izumi, F.; Iyi, N.; Sasaki, T. *J. Am. Chem. Soc.* **2008**, *130*, 16344−16350. (e) Woodward, J. D.; Almond, P. M.; Albrecht-Schmitt, T. E. *J. Solid State Chem.* **2004**, *177*, 3971−3976. (f) Wang, S.; Alekseev, E. V.; Depmeier, W.; Albrecht-Schmitt, T. E. *Inorg. Chem.* **2012**, *51*, 7−9.

(19) (a) Brese, N. E.; O'Keeffe, M. *Acta Crystallogr., Sect. B* **1991**, *47*, 192−197. (b) Roulhac, P. L.; Palenik, G. J. *Inorg. Chem.* **2002**, *42*, 118−121.

(20) (a) Carnall, W. T.; Fields, P. R.; Pappalar, R. G. *J. Chem. Phys.* **1970**, *53*, 2922−2938. (b) Carnall, W. T.; Liu, G. K.; Williams, C. W.; Reid, M. F. *J. Chem. Phys.* **1991**, *95*, 7194−7203.

(21) Bregiroux, D.; Terra, O.; Audubert, F.; Dacheux, N.; Serin, V.; Podor, R.; Bernache-Assollant, D. *Inorg. Chem.* **2007**, *46*, 10372−10382.